

# Mechanism for Materializing Wave Effects

Eduardo V. Flores<sup>1</sup>

Department of Physics & Astronomy  
Rowan University  
Glassboro, NJ 08028

We reveal that the mechanism driving the manifestation of wave effects is fundamentally embedded within quantum field theory. These wave effects become real when conservation laws are satisfied, allowing quantum effects to fully materialize, and remain virtual when these laws are violated. The materialization process is governed by external sources that supply conserved quantities, and by virtual particles that carry these quantities. For example, a photon in a region of constructive and destructive interference can form either a real or virtual interference pattern, contingent on the availability of these conserved quantities. Our findings also resolve a longstanding paradox in an experiment that challenges the principle of complementarity. Furthermore, we predict that low-energy galactic neutrinos, constrained by the limited range of vector boson interactions, behave as a classical ideal gas—a prediction we believe is experimentally testable. These insights not only address fundamental questions in quantum mechanics but also open new avenues for future exploration.

**Key Words:** virtual particles, conservation laws, principle of complementarity, galactic neutrinos

## Introduction

As a particle propagates, an uncountable number of virtual quantum effects occur. For example, a free photon can decay into a virtual electron-positron pair, but since this would violate momentum conservation, it remains virtual. The virtual electron might produce a virtual neutrino and vector boson, which then recombine into the virtual electron, and so forth. The virtual possibilities within quantum fields are endless. Interestingly, even though the charm quark has a heavier mass than a proton, virtual charm quarks can still appear within a proton [1]. All of these virtual processes contribute to the calculations of net physical processes, and in this sense, they possess a certain element of reality. However, none of these virtual quantum processes can materialize if a conservation law is violated.

When conservation laws are fulfilled, there is a probability that virtual processes may materialize. For example, a high-energy photon could decay into a real electron and positron, provided that an external object, such as the nucleus of an atom, is present to supply the necessary momentum, thereby satisfying momentum conservation. Similarly, when two waves interfere, they may produce regions of constructive and destructive interference. If the conservation laws are met, it is likely that the particles associated with these waves will conform to the pattern of constructive and destructive interference; we refer to this as a

---

<sup>1</sup> Email: flores@rowan.edu

real wave effect. In this work, we highlight a case where the formation of an interference pattern cannot materialize due to a violation of conservation laws; we refer to this as a virtual wave effect.

Aside from gravitational effects, the development of all matter and radiation can be studied using quantum physics alone. When particles interact, they exchange conserved quantities. The stability of the hydrogen atom requires a continuous exchange of energy and momentum between the proton and electron. Similarly, fermion degeneracy pressure, which is responsible for the formation of neutron stars, white dwarfs, and other compact objects, relies on the exchange of energy and momentum. In quantum physics, particles interact with one another through virtual particles [2]. Therefore, the properties of virtual particles play a key role in the formation of quantum effects.

The fundamental energy-momentum relation for free particles,  $E^2 = p^2c^2 + m^2c^4$ , is the foundation of the wave equations that these particles obey. It is important to note that virtual particles do not adhere to this energy-momentum relation [3]. As a result, virtual particles exhibit a range of unusual properties: they cannot be set free, they may exist only briefly, they may be superluminal, and they can transfer either a pull or a push. Another significant property of a virtual particle is its range of interaction. The range of interaction for a virtual photon is infinite, while the range for a virtual massive vector boson is on the order of  $10^{-18}$  meters. In addition to transferring energy and momentum, virtual particles can also transfer other conserved quantities, such as angular momentum and charge.

We can study the hydrogen atom using the Dirac equation. The accuracy of the Dirac equation in predicting the behavior of the hydrogen atom is largely due to the significant mass difference between the electron and the proton [4]. The heavy proton is minimally affected by the motion of the electron, leading to excellent predictions for nearly all energy levels. However, in 1947, the Lamb-Rutherford measurement of the hydrogen atom fine structure confirmed an upward shift of the  $2S_{1/2}$  levels relative to the  $2P_{1/2}$  lines [b]. This "Lamb shift" arises from the interaction of electrons with the fluctuations of quantized radiation fields. Calculating the Lamb shift requires the use of quantum electrodynamics (QED). QED introduces virtual particles as a means of transferring conserved quantities between interacting particles. The basic interaction in QED is described by the Feynman diagram in Fig. 1, where a photon interacts with an electron. It is important to note that all other interactions in QED are built upon this fundamental interaction [b].

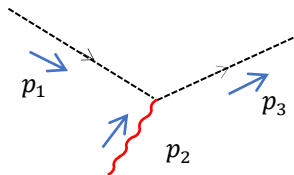


**Fig. 1 Basic Feynman diagram in quantum electrodynamics.** An electron interacts with a photon. This interaction gives rise to all other interactions in QED.

In cases where the masses of the bound state particles are comparable, such as in positronium, the Dirac equation, which works so well for hydrogen, fails to produce the correct energy spectrum. An approach based on the exchange of virtual particles is required to reproduce experimental results [4]. Key effects in positronium are obtained by using basic interactions an infinite number of times. For problems concerning

the positronium spectrum, the ladder prescription is sufficient. In this approximation, a Lorentz frame can be found in which only one virtual photon is exchanged at a given time, but this process can be repeated an arbitrary number of times. However, it is important to recognize that there are a multitude of possible diagrams. In other words, the electron and positron exchange an infinite number of virtual photons. This can be understood by realizing that the electron and positron in a bound state spend a relatively long time close to each other, interacting many times. Additionally, each virtual photon contributes just a small amount to maintaining the bound state. The effectiveness of this approach is demonstrated by its success [4]. Thus, for bound state systems, the approach based on the exchange of virtual particles appears to be more general than the direct application of the Dirac equation.

As an application of our observations, we present a resolution of an experiment that challenges the principle of complementarity [5]. The wave-particle duality is an expression of complementarity. It is well-known that the which-way information,  $K$ , is a particle property, and visibility,  $V$ , is a wave property. Both of these values are limited by the principle of complementarity, which is expressed by the inequality [6,7]:

$$K^2 + V^2 \leq 1. \quad (1)$$

Inspired by Wheeler's work, we can associate the which-way information,  $K$ , with our ability to identify the origin of a particle by applying the principle of momentum conservation [8]. By detecting the final position and direction of a free particle, we can deduce where it originated. When we can accurately determine the particle's origin, we have maximum which-way information,  $K = 1$ . If we cannot identify the particle's origin, we have zero which-way information,  $K = 0$ . Additionally, we can have partial which-way information,  $1 > K > 0$ .

On the other hand, visibility,  $V$ , measures the contrast between bright and dark fringes in an interference pattern formed by the accumulation of particles. If a particle avoids a particular region and is attracted to an adjacent region, it contributes to the formation of adjacent dark and bright fringes, and its visibility is maximum,  $V = 1$ . If a particle is equally likely to reach any point within a region, it contributes to the formation of a uniform distribution, and its visibility is zero,  $V = 0$ . We can also have partial visibility,  $1 > V > 0$ .

### **Virtual and Real Interference**

Consider a low intensity photon beam that is split into two beams. The resulting beams are redirected to cross at a small angle and interfere, as depicted in Figure 2. The photon beams can be treated as two plane waves, in phase, that intersect at a small angle  $\alpha$ , and produce an electric field intensity proportional to  $E_0^2(1 + \cos[2\pi\alpha y/\lambda])$ , where  $y$  represents the transverse location and  $\lambda$  is the wavelength. Therefore, in the experiment depicted in Fig. 2, the electric field exhibits constructive and destructive wave interference in the region where the beams intersect.

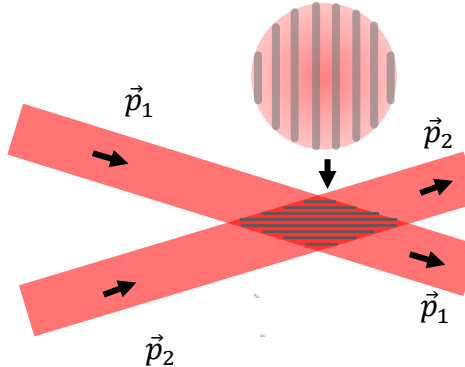


**Fig. 2 Two beams in phase intersect.** Two low-intensity photon beams, in phase, intersect and pass through each other unperturbed. At the region of intersection, the electric field exhibits both constructive and destructive interference. The circle above the beams illustrates the cross-section of the interference pattern. Since the beams pass through each other freely, the energy and momentum of the photons must remain undisturbed from the beginning to the end of each beam.

The electric field at the beam intersection has regions of constructive and destructive interference. However, conservation laws prevent the photon from aligning itself with the electric field. As a photon crosses the beam intersection, its conserved quantities must remain unchanged due to these laws. The absence of external sources at the beam intersection makes it impossible for virtual particles to transfer the necessary momentum to move the photon from a dark fringe to a bright fringe. This is especially true when the intensity is so low that, on average, there is only one photon in the entire setup.

We might assume that during short periods of time, conservation laws could be violated. Perhaps, for brief moments, a photon could be deflected from a region of destructive interference to a region of constructive interference without requiring virtual particles to transfer momentum from external sources. However, once this deflection occurs, there would be a permanent change in the photon's angular momentum relative to a fixed observer.

In the experiment depicted in Fig. 2, the time it takes for a photon to cross the beam intersection appears to be short. Thus, as the photon crosses the intersection, it might follow the interference pattern in the electric field for a brief duration. However, we could make the two beams arbitrarily wide and the angle of intersection  $\alpha$  arbitrarily small. In this case, the beam intersection could be made arbitrarily long, meaning the duration during which the photon's conserved quantities are violated could also be arbitrarily long. Therefore, if the photon were to follow the regions of constructive and destructive interference in the electric field, we could end up violating a conservation law for an arbitrarily long period.

We conclude that while a free photon passes through the beam intersection, it cannot simultaneously follow the electric field conditions and maintain its conserved quantities unaltered. This leads us to conclude that the constructive and destructive electric field interference is a virtual wave effect. By 'virtual,' we mean that the photon cannot adhere to its associated electric field and instead acts as a free particle. The photon crosses the beam intersection as a free particle.

The principle of complementarity agrees with the notion of a virtual interference. A photon detector may be placed at the end of each beam in Fig. 2. Since at the beam intersection there is no obstacle for a photon

going through, then once a detector clicks, the path and origin of the photon is revealed uniquely, given full which way information, ( $K = 1$ ). Thus, according to the principle of complementarity, a photon cannot conform to the constructive and destructive interference pattern in its associated electric field; thus, the interference pattern must be virtual, ( $V = 0$ ). We note that in classical electrodynamics, electric field interference is always a real effect ( $V = 1$ ); therefore, according to classical electrodynamics, in the experiment in Fig. 2, there is a violation of the complementarity inequality, as  $K^2 + V^2 = 2$ .

Virtual particles in hydrogen not only maintain the electron bound to the proton but are also responsible for every quantum effect observed. Let us consider the electron in hydrogen with quantum numbers  $n = 4$ ,  $l = 1$ , and  $m = 0$ . In this state, the electron's radial probability density displays a pattern with alternating high and low-intensity regions. The radial probability density is in principle an observable effect. This pattern is formed as the electron is driven by, perhaps an infinite number of, virtual particles from low-intensity regions to high-intensity regions. We note that these regions of high and low intensity are similar to the bright and dark fringes observed in interference patterns of light. We infer that the photon must also be driven by virtual particles from low to high-intensity regions in the formation of a real interference pattern on a screen as seen in Fig. 3. We note that when the photon rate is so low that on average only one photon is present in the entire setup, the interference pattern is formed one photon at a time. We also note that a version of this experiment was conducted and analyzed by Pfleegor and Mandel [9], and others [10,11].

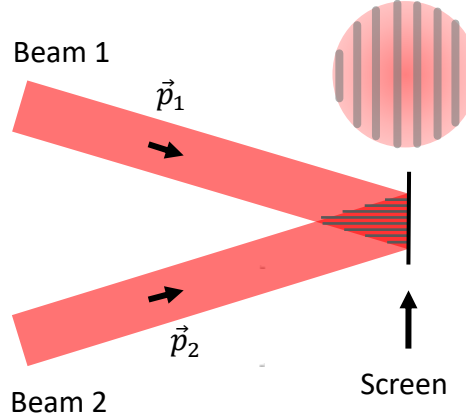


**Fig. 3 Real interference pattern on a screen.** Two low-intensity photon beams, in phase, intersect and converge on a screen. At the region of intersection, the electric field associated with the beams undergoes constructive and destructive interference. Virtual particles must transfer momentum from screen to incoming photon so that the photon follows the characteristic pattern of fringes seen on the screen.

For a photon to form a real interference pattern on a screen, it must interact with the screen at a distance. The screen consists of positive and negative charges. The fundamental Feynman diagram that describes how a photon interacts at a distance with a charge is depicted in Fig. 4. This process is known as Delbrück scattering [12]. Delbrück scattering has been observed with photons in the MeV range [13]. An incoming photon with momentum  $\vec{p}_1$  interacts with a virtual electron in a closed loop. The two photon lines, ending with an 'x' and having momenta  $\vec{p}_2$  and  $\vec{p}_4$  represent the Coulomb field of a charge. Since this interaction occurs twice, the amplitude for this interaction is proportional to the square of the charge. Therefore, at

the most basic level, the interaction of a photon with a positive or negative charge over a distance is identical. The outgoing photon emerges with momentum  $\vec{p}_3$ .

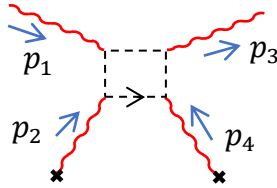


**Fig. 4 Scattering of light by light.** The most basic interaction of a photon with the Coulomb potential of a charge is described by this Feynman diagram. A photon with momentum  $\vec{p}_1$  interacts with a virtual electron loop. Virtual photons that represent the Coulomb field are depicted by the curved lines ending at an 'x'. These virtual photons also interact with the virtual electron loop. A real photon emerges with momentum  $\vec{p}_3$ .

The scattering of light by light in Fig. 4 is actually very weak for visible light [14,15]. Visible light is in the low frequency range, and the cross section for scattering of visible light from a Coulomb potential is proportional to  $(Z\alpha)^4 r_0^2 (\hbar\omega/mc^2)^4$  where  $\hbar\omega \ll mc^2$  [15]. Here,  $Z$  is the number of charges producing the Coulomb field,  $\alpha$  is the fine structure constant,  $r_0$  is the classical radius of the electron,  $\omega$  is the angular frequency of light and  $m$  is the electron mass. In other words, it is very unlikely for visible light to be scattered by electric charge. However, we recall the positronium case which requires an infinite number of virtual particle exchanges to keep the electron and positron bounded. The photon case appears to be similar, there must be an infinite number of virtual particle interactions, like the one in Fig. 4, between photon and charge to transfer enough energy-momentum to deflect the photon in order to fulfill the interference pattern.

A study using the Euler-Heisenberg effective Lagrangian [16,17] shows that for low-energy photons, photon momentum deflection is much greater than that predicted by Delbrück scattering alone [18,19]. The Euler-Heisenberg effective Lagrangian encapsulates the interactions of light at the one-loop level in the low-energy region. The author of Ref. [19] explains why the Euler-Heisenberg effective Lagrangian involves an infinite number of virtual particle exchanges. Additionally, a photon approaching the screen can simultaneously interact with a macroscopic number of positive and negative charges that make up the screen, overcoming the weakness of individual interactions and enabling the formation of the interference pattern on the screen. We are not aware of any other mechanism in QED through which a macroscopic object can transfer energy-momentum to a photon at a distance, allowing it to become part of a real interference pattern.

### Complementarity Challenged

Returning to the setup in Fig. 2, we reconsider the two in-phase laser beams that cross at a small angle, then separate and ultimately end up at detectors, as depicted in Fig. 5. The experiment could be conducted with a low photon count, such that there is a high probability of only one photon being present in the entire setup at any given time. When two in-phase plane waves intersect at a small angle, the electric field exhibits constructive and destructive interference fringes in the region where the beams intersect.

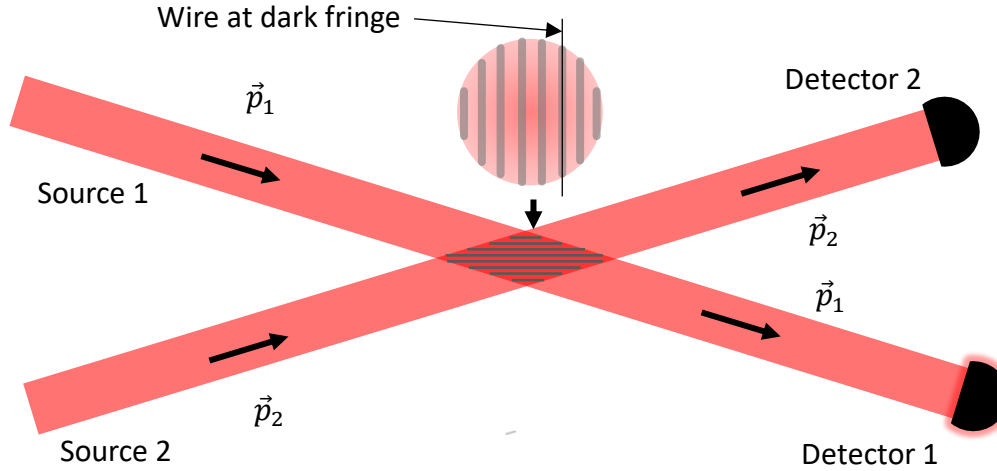


**Fig. 5 Two coherent beams intersect and end at detectors.** Two low-intensity, in-phase laser beams intersect and ultimately end up at detectors. When detector 1 clicks, we can infer with certainty that the photon came from source 1, meaning the which-way information is maximized ( $K = 1$ ). At the intersection of the beams, the electric field undergoes both constructive and destructive interference, resulting in a characteristic fringe pattern. A wire placed at the center of a dark fringe does not alter the photon count at the end detectors, indicating the presence of a real dark fringe with high visibility ( $V = 1$ ).

Using the setup in Figure 5, the authors of the experiment in Ref. 20 aimed to measure both the visibility and which-way information simultaneously. To accomplish this, they employed a technique originally introduced by S. S. Afshar [5]. In this technique, a wire that is 12.5 times thinner than the distance between consecutive bright or dark fringes is scanned across the intersection region of the beams. First, they consider the case where the beams cross freely and establish the photon count at the end detectors. Next, under similar conditions, the  $17 \mu\text{m}$  thick wire is scanned across the beam intersection. The ratio ( $f$ ) of the photon count with the wire in place over the photon count without the wire is plotted in Figure 6. The solid line represents a calculation of  $f$  using Fraunhofer diffraction [20]. We note that theoretical and experimental results are in excellent agreement.

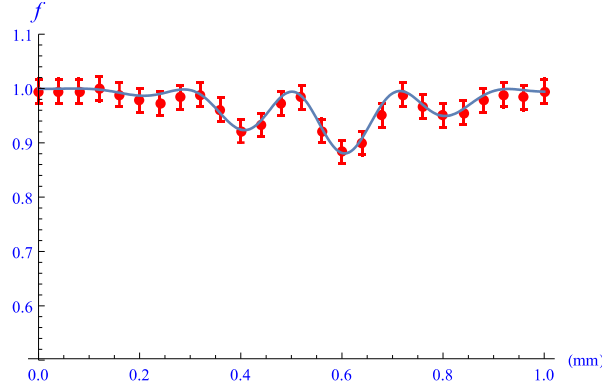


**Fig. 6 Fraction of photon count ( $f$ ) at end detector.** This plot displays the fraction of photon count at one of the end detectors as a  $17 \mu\text{m}$  thick wire is scanned across the  $1.0 \text{ mm}$  beam intersection. The error bars in the plot represent statistical uncertainties, while the solid line represents the theoretical prediction using Fraunhofer diffraction. Remarkably, there is evidence that these results do not change even when the experiment is conducted at an average separation between one photon and the next of  $3 \text{ km}$  [20].

By analyzing Figure 6, it can be observed that the fraction of photon count decreases to 0.88 when the  $17 \mu\text{m}$  thick wire is positioned at  $0.6 \text{ mm}$ , suggesting the existence of a bright fringe at this location. This reduction in the photon count corresponds to a 12% decrease in the total number of photons since they have been either absorbed or scattered by the wire. Conversely, when the wire is placed at  $0.72 \text{ mm}$ , the fraction of photon count remains close to one, indicating that no photon losses occur at this position. These observations indicate that the wire can significantly affect the photon count, and the position of the wire can be used to determine the presence or absence of real interference fringes.

In classical physics, the interference pattern at the beam intersection is present regardless of whether we measure it or not. Thus, when the wire is placed at  $0.72 \text{ mm}$ , at the center of a dark fringe, there are no losses due to wire diffraction because there is no field to diffract. If there is no wire diffraction, the which-way information is maintained ( $K \approx 1$ ). Thus, photons that come from source 1 (2) will most likely end up at detector 1 (2). Since there is no light at the wire, the intensity at the wire is zero ( $I_0 \approx 0$ ). Light has been deflected to a nearby bright region where the intensity is nonzero ( $I \neq 0$ ). As a result, the visibility in this region is 1 ( $V = \frac{I-I_0}{I+I_0} \approx 1$ ). Thus, the complementarity inequality in Eq. 1 appears to be violated, as  $K^2 + V^2 \approx 2$ .

Similarly, in the Afshar experiment, comparable results were obtained and published [5]. However, instead of a single wire, a wire grid was used. It is worth noting that some authors have claimed to resolve the paradoxical results of the Afshar experiment using grid diffraction analysis [21,22]. We have argued elsewhere that grid diffraction analysis does not resolve the paradox of Afshar's experiment [23]. In fact, wire grid diffraction analysis does show two very small bumps, one at each detector. The light in these bumps is the result of diffraction, which causes the light to lose its which-way information. Nevertheless, it has been estimated that only 1 in 100,000 photons reaching a detector have lost their which-way information due to wire grid diffraction [24].

## Resolution of Paradox

We find that if an interference pattern were to materialize by itself at the beam intersection in Fig. 5, as in classical physics, the principle of complementarity and conservation laws would be violated. Since these principles cannot be violated, we propose that the wire materializes the interference pattern at its location. QED provides the mechanism for this materialization. As a photon approaches the wire, it interacts with the charges that make up the wire through virtual particle processes as the one in Fig. 4. Virtual particles maneuver the photon away from regions of low electric field intensity and toward regions of higher electric field intensity.

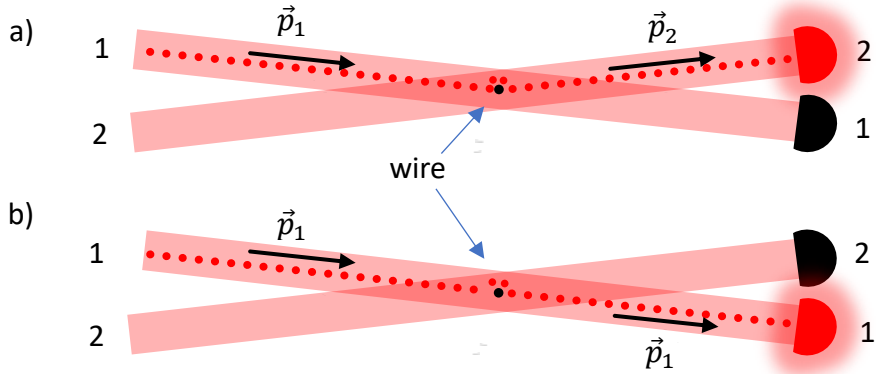


**Fig. 7 Wire at the center of a dark fringe.** Assuming a photon emitted from source 1 is heading toward the wire located at the center of a dark fringe, the photon is guided around the wire, contributing to the formation of the dark fringe. Beyond the wire, the photon encounters two identical beams: a) beam 2, which requires the photon to acquire momentum  $\vec{p}_2$ , and b) beam 1, which requires the photon to acquire momentum  $\vec{p}_1$ . The wire, through virtual particles, must provide the momentum needed for these maneuvers.

When a photon approaches the wire and is guided around it by a transfer of rather large momentum from the wire, it achieves maximum visibility,  $V = 1$ , as it contributes to the formation of adjacent dark and bright fringes. After the deflection, the photon encounters two outgoing beams with identical electric field intensities. It is important to note that the momentum required for the photon to enter each beam is different: either  $\vec{p}_1$  or  $\vec{p}_2$ . Classical wire scattering cannot provide the correct momentum, which can only be either  $\vec{p}_1$  or  $\vec{p}_2$ . The momentum must be transferred from the wire to the photon by virtual particles.

Due to the nature of quantum mechanics, the photon randomly takes one of the two equally likely beams. This random process erases the which-way information,  $K = 0$ , as we can no longer determine whether the photon originated from source 1 or 2. This mechanism also ensures that the photon count at the end detectors remains unchanged, as observed in the experiment. In summary, at the wire, the visibility of the photon is 1, while its which-way information is 0, and the complementarity inequality in Eq. 1 is preserved.

We note that without the mechanism depicted in Fig. 4 for transferring energy-momentum from the wire to the photon, the complementarity inequality would be violated. This mechanism is a part of QED. In contrast, according to classical electrodynamics, the complementarity inequality is violated in both the

experiment in Fig. 2 and the experiment in Fig. 5. Therefore, the paradoxical findings in the Afshar experiment can only be resolved within the framework of QED.

### Non-relativistic Galactic Neutrinos

Neutrinos and antineutrinos experience an attractive force and can annihilate into different particles depending on their energy. However, very low-energy neutrinos and antineutrinos can only annihilate into photons, although this cross section is extremely small [25]. Thus, if a low-energy neutrino and antineutrino meet, they experience attraction and tend to form a stable atom. However, the uncertainty principle indicates that these low-mass, low-energy particles cannot be confined within the  $10^{-18}$  m range of the weak interaction; thus, they quickly separate as free particles. Similarly, any two neutrinos will not interact if they are separated by distances greater than  $10^{-18}$  m.

The net wavefunction of an electron gas in a metal is antisymmetric. Consequently, wave effects, such as Fermi pressure, are realized by the transfer of energy and momentum among electrons through virtual particles, which have a range that covers the entire metal. Similarly, the net wavefunction of a neutrino gas is also antisymmetric. However, if the separation between neutrinos is greater than  $10^{-18}$  m, wave effects remain virtual because virtual vector bosons do not reach far enough to transport energy-momentum and thus cannot materialize wave effects. In this case, neutrinos behave as free particles, governed solely by conservation laws. This situation is similar to that in Fig. 2, where the electric field associated with a photon exhibits constructive and destructive interference. However, the photon must disregard the state of its associated electric field and travel as a free particle, guided only by conservation laws.

For the sake of calculation, we might assume that non-relativistic neutrinos in the galaxy are the main component of dark matter. We may assume an average neutrinos mass of  $m = 0.1 \text{ eV}/c^2$  [26] and consider the density of dark matter at the solar system to be  $10^{-21} \text{ kg}/\text{m}^3$  which translates into  $n = 5.6 \times 10^{15}$  neutrinos per cubic meter. We could consider non-relativistic galactic neutrinos bound by the gravitational field of the Milky-Way galaxy. The escape velocity of a particle starting at the solar system is estimated to be [27]  $v_e \approx 550 \text{ km/s}$ , then neutrino temperature at the solar system should be lower than  $T = \frac{mv^2}{3k_B} \approx 1.3 \text{ mK}$  to stay bounded. These particles mean free path is

$$\lambda = \frac{1}{\sqrt{2\pi}d^2n} \approx 4 \times 10^{19} \text{ m}$$

where  $d \approx 10^{-18}$  m is the effective range of interaction of a neutrino and  $n = 5.6 \times 10^{15}$  is the particle density. If Sedna, the most distant observable object in the solar system, is used, the diameter of the solar system is  $2.9 \times 10^{14}$  m. A neutrino would travel the distance of hundred thousand solar systems before it interacts with another neutrino. We may safely treat non-relativistic galactic neutrinos as a classical ideal gas with negligible viscosity.

It would be very difficult to test in a lab whether diluted non-relativistic neutrinos behave as an ideal gas with no viscosity. However, we could model dark matter in a galaxy as an ideal gas of neutrinos and antineutrinos. This would require using Euler's equation for inviscid fluids and the ideal gas law. We could then test whether this model fits observational data.

## Final Remarks

Virtual particles in a hydrogen atom not only bind the electron to the proton but also account for all quantum effects predicted by the Dirac equation. The solution to the Dirac equation is expressed as a specific wavefunction, which defines the possible actions of virtual particles. The wavefunction serves as a blueprint, while the virtual particles carry out the quantum processes. However, if conservation laws are not fulfilled, these processes cannot materialize. Understanding the mechanism through which quantum effects manifest could offer deeper insights into quantum physics. We have identified a mechanism, already embedded in quantum field theory, that substantiates the wavefunction. Notably, this mechanism resolves a paradox and leads to a testable prediction about neutrinos. These findings could enhance our understanding of quantum physics, especially the wave-particle duality paradox.

## References

- [1] R. D. Ball, et al., *Nature*, 608, pages483–487 (2022)
- [2] J. D. Bjorken & S. D. Drell, *Relativistic Quantum Mechanics* (McGraw-Hill, New York, 1964).
- [3] M. J. G. Veltman, *Facts and Mysteries in Elementary Particle Physics* (World Sci. Ltd., 2003), p. 254
- [4] W. Greiner and J. Reinhardt, *Quantum Electrodynamics* (Springer, 2009), Fourth Edition
- [5] S. S. Afshar, E. V. Flores, K. F. McDonald, E. Knoesel, *Found. Phys.*, 37 (2) 295-305 (2007)
- [6] D. Greenberger and A. Yasin, *Phys. Lett. A* 128, 391 (1988)
- [7] B.-G. Englert, *Phys. Rev. Lett.* 77 2154 (1996)
- [8] J. A. Wheeler, in *Quantum Theory and Measurement* (Princeton University Press, 1983)
- [9] Pfleegor, R. L. & Mandel, L., *Phys. Rev.* **159**, 1084-1088 (1967)
- [10] Radloff, W. *Ann. Phys. (Leipzig)* **26** (1971)
- [11] Louradour, F., Reynaud, F., Colombeau, B. & Froehly, C., *Am. J. Phys.* **61**, 242 (1993)
- [12] M. Delbrück, *Zeits. Phys.*, 84, 144 (1933)
- [13] M. Schumacher, I. Borchert, F. Smend, and P. Rullhusen, *Phys. Lett.* 59B, 134 (1975).
- [14] R. Karplus & M. Neuman, *Phys. Rev.* 83, 776 (1951)
- [15] V. Costantini, B. De Tollis and G. Pistoni, *Nuovo Cimento*, 2, 733 (1971)
- [16] W. Heisenberg and H. Euler, *Z. Phys.* 98, 714 (1936), arXiv:physics/0605038 [physics]
- [17] J. S. Schwinger, *Phys. Rev.* 82, 664 (1951), [,116(1951)]
- [18] J. Y. Kim & T. Lee, *Mod. Phys. Lett. A*, Vol. 26, No. 20 (2011) pp. 1481-1485 arXiv:1012.1134v2
- [19] T. Lee, arXiv:1711.00160v2 (2018)
- [20] E. V. Flores, J. Scaturro, arXiv:1412.1077v4
- [21] Steuernagel, O., *Found. Phys.* 37, 37: 1370–1385 (2007)
- [22] V. Jacques, N. D. Lai, A. Dreau, D. Zheng, D. Chauvat, F. Treussart, P. Grangier, J-F Roch, *New J. Phys.* 10, 123009 (2008)
- [23] E. Flores, *Found. Phys.* 38, 778- 781 (2008)
- [24] Flores, <https://arxiv.org/pdf/0803.2192>
- [25] T. De Graaf, H.A. Tolhoek, *Nuclear Physics* 81, 3 (1966)
- [26] The KATRIN Collaboration. *Nat. Phys.* 18, 160–166 (2022)
- [27] Kafle, P.R.; Sharma, S.; Lewis, G.F.; Bland-Hawthorn, J. (2014). *The Astrophysical Journal*. 794 (1): 17